Materials Research Proceedings 41 (2024) 1426-1435 https://doi.org/10.21741/9781644903131-158

Improving the flow forming process by a novel closed-loop control

KERSTING Lukas[1,a,*], SANDER Sebastian[1], ARIAN Bahman[2,b], ROZO VASQUEZ Julian[3,c], TRÄCHTLER Ansgar[1,4], HOMBERG Werner[2] and WALTHER Frank[3]

[1]Fraunhofer Institute for Mechatronic Systems Design (IEM), Paderborn, Germany

[2]Paderborn University, Forming and Machining technology (LUF), Germany

[3]TU Dortmund University, Chair of Materials Test Engineering (WPT), Germany

[4]Heinz Nixdorf Institute (HNI), Paderborn University, Germany

[a]lukas.kersting@iem.fraunhofer.de; [b]ba@luf.uni-paderborn.de, [c]julian.rozo@tu-dortmund.de

Keywords: Flow Forming, Closed-Loop Control, Model-Based Control Design

Abstract. The incremental flow forming process is currently enhanced in research context by special closed-loop property control concepts to increase the productivity and to control the product properties making invisible property structures like a magnetic barcode possible. However, it is preferred to establish property control concepts on single roller machines instead of conventional machines with three roller actuation due to the better machine accessibility. For those single roller machines, rather poor surface qualities of flow formed workpieces were observed in the past especially for hydraulic actuators. Thus, a new actuator closed-loop position control concept is developed in this paper using model-based control design methods and taking the flow forming forces as a load into account. The novel closed-loop control is validated during workpiece production at the actual single roller flow forming machine. An analysis of the manufactured workpieces show that the surface quality is significantly enhanced by the new control to a roughness level almost similar to conventional three roller flow forming. Thus, a sincere added value to the flow forming process is offered by the novel actuator closed-loop position control.

Introduction

In the incremental flow forming process, it is currently difficult to control the resulting product properties and microstructure due to the large number of disturbance variables from the semifinished part and the environment (e.g. temperature, tool and machine behavior) [1]. A promising research approach to reproducibly set the properties and microstructure during flow forming despite disturbances is closed-loop property control (see [1]). In such closed-loop property control, material properties and the workpiece geometry are automatically controlled by online measurement and an online adaptation of the roller tool trajectory. The term ‘closed-loop property control’ also implies special requirements for the flow forming machine. First, the actuator dynamics have to be fast enough to change the process parameters depending on the control signal. Second, the machine control has to be accessible by an external control signal from the online property sensors so that the process parameters can be changed, e.g. by using a control prototyping system. Third, online property sensors must be placed near the roller tool for in-situ measurements at the forming zone. For this reason, single roller flow forming machines are preferred for use in closed-loop property control since there is more installation space for the property sensors than in conventional three roller machines. However, in previous research by the authors, a rather poor surface quality of workpieces manufactured by a hydraulic single roller flow forming machine was observed [2, 3]. The reason is that the existing machine control on a rapid control prototyping system does not consider the special load induced by single roller flow forming. For this purpose,

this paper presents the development of a novel closed-loop position control for a single roller flow forming machine as an extension to the existing control. To especially take the requirements for property-controlled flow forming into account, a model-based development approach for hydraulic systems was chosen. The selected approach has already been successfully applied to design closed-loop controls for hydraulic robot systems [4] and HiL axle test rigs [5], but to our knowledge it has never been applied to a property-controlled single roller flow forming machine.

Process and machine setup

Property-controlled flow forming. This paper focusses on the reverse flow forming of tubular parts made from metastable austenitic stainless steel AISI 304L. In the process, the semifinished part is fastened on a rotating mandrel. During the metal forming, a roller tool is moved by a flow forming actuator with a defined feed rate f in axial x direction and infeed Δr in radial y direction alongside the workpiece. This leads to a wall thickness reduction Δw (plastic deformation) and to a strain-induced α'-martensite formation in the workpiece. To ensure that wall thickness and α'-martensite match to a desired value, a closed-loop property control is appropriate (see Fig. 1).

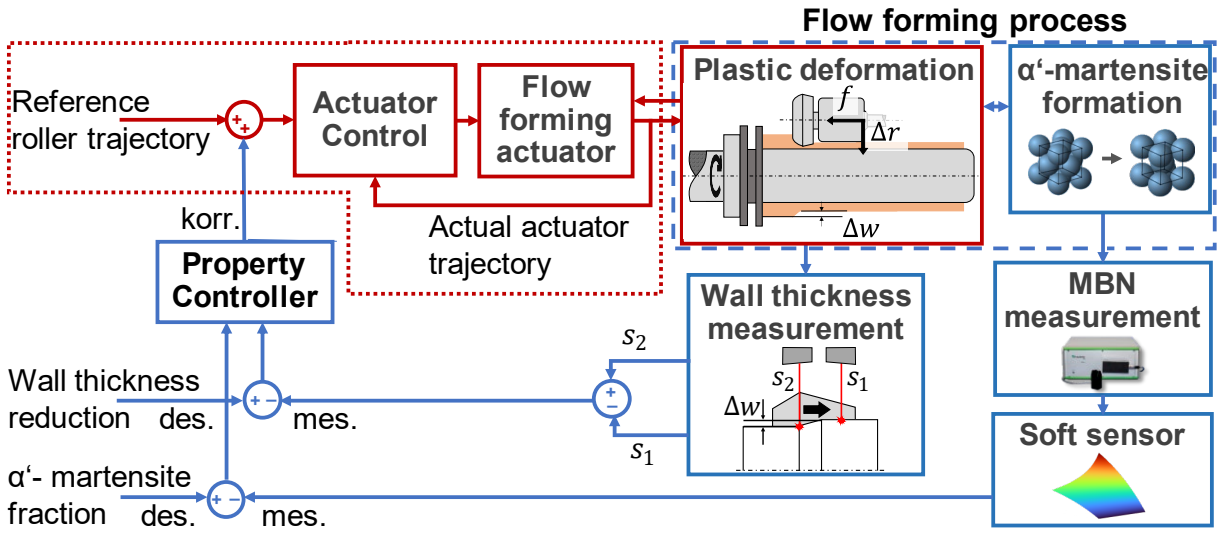

Fig. 1. Property-controlled flow forming process including actuator control

Here, the wall thickness reduction can be measured online by two laser distance sensors. The α'-martensite fraction is determined by a combined approach with a magnetic Barkhausen noise (MBN) measurement and a so-called soft sensor. Both sensor signals are compared to desired values and processed by a property controller. The property controller corrects the reference roller trajectory given by the machine control. The corrected trajectory leads to a change of f and Δr and thus to change of Δw and α'-martensite. At this point, it is essential to ensure that the tool trajectory actually corresponds the to the desired trajectory from the property control. For this reason, the flow forming actuator is equipped with an actuator control system which is the system of interest in this paper (highlighted in red in Fig. 1). For further information concerning the closed-loop property control, it is referred to the literature (e.g. [1]) since it is out of scope of this paper.

Actuator and machine setup. In this paper**,** the flow forming machine PLB 400 from Leifeld Metal Spinning GmbH is used. This machine basically features a cross support actuator with the roller tool, a spindle-driven mandrel carrying the workpiece and a dual roller counterholder placed opposite to the roller tool to avoid mandrel deflection by ensuring a force balance (see [2]). The cross support, which is in focus of this paper, consists of two parts: a lower machine support actuator (x axis) that is hydraulically moved in axial x direction with a certain feed $f = \dot{x}_p$ (velocity) and an upper machine support actuator (y axis) that is mounted on the lower part. The upper machine support actuator is rigidly connected to the roller tool and can be hydraulically

moved in radial y direction to realize a certain infeed Δr to the workpiece. The setup and functionality of the two machine support axis is more detailly explained in Fig. 2.

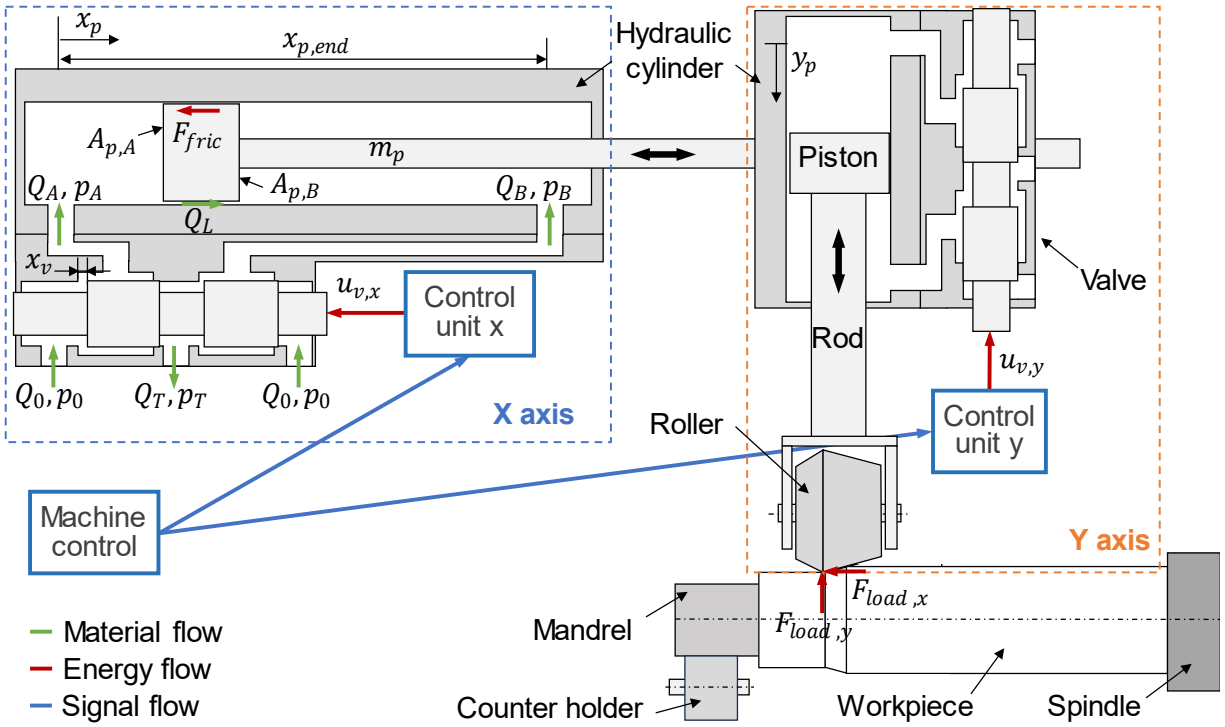

Fig. 2. System structure of the flow forming machine

Each hydraulic machine support axis is composed of a hydraulic cylinder and a proportional valve (Bosch Rexroth 4WRPEH) that controls the volume flow from the pump to the cylinder leading to the piston motion. The valve opening and thus the volume flow is continuously adjustable depending on the input voltage $u_{v,x}$ or $u_{v,y}$ (within a range of 0 – 10 V). The input voltages $u_{v,x}$ and $u_{v,y}$ are generated by the machine control. The machine control is realised on the rapid control prototyping system NI cRIO 9035. The LabVIEW-based control software was originally developed by *Hornjak* and *Lossen* in [6, 7] for friction spinning purposes. It can be separated into a main control, with a user interface and software interface to the property control system (see [8]), and one control unit per axis. In each control unit, $u_{v,x}$ and $u_{v,y}$ are generated by the actuator control. The current actuator control is a mixed open-loop setup with position feedback. Depending on the desired piston velocity, a certain value of $u_{v,x}$ and $u_{v,y}$ is applied from a dataset as long until the desired piston position is reached. For this purpose, the piston positions are measured with a magnetostrictive transducer (MTS Temposonic E101) and fed back to the control. However, the current actuator control is limited concerning the use during flow forming since the forming forces are much higher like in friction spinning. This leads to inaccuracies concerning the voltage datasets. Thus, the both control units are redesigned in this paper to a full closed-loop control.

Methodology

To develop the new closed-loop for the hydraulic actuator system, a model-based development approach for control design was chosen. Here, the controller is first designed using a simulation model and subsequently applied to the actual system. Thus, the closed-loop control can be developed time-efficiently with a good control performance. The model-based development procedure includes four steps and milestones. First, an analytic system model is created that represents the dynamic behaviour of the system to be controlled (1). The model is implemented in a simulation environment and parameterized using experimental data (2). Subsequently, the

control is developed and tested virtually using the model and suitable controller parameter are selected (3). Finally, the developed control is implemented in the machine control and validated at the actual machine (4). This procedure is applied in the following to the hydraulic actuator system.

Modelling

A simulation model was created in MATLAB/Simulink to describe the static and dynamical transfer behavior of the hydraulic machine support actuators. For this purpose, a hydraulic model by [5] and [8] was adapted. Since the machine supports in x and y direction have an identical structure, albeit with different dimensions and loads, the model is exemplary described for the x axis in the following. The overall model is structured according to the components of the real machine into a valve and a cylinder model (Fig. 3). The model additionally includes an external load model that is specifically designed for the machine application in flow forming. In the following, the models and their adaption to the flow forming machine are further described. However, for the full model equations of the hydraulic system it is referred to the literature [8].

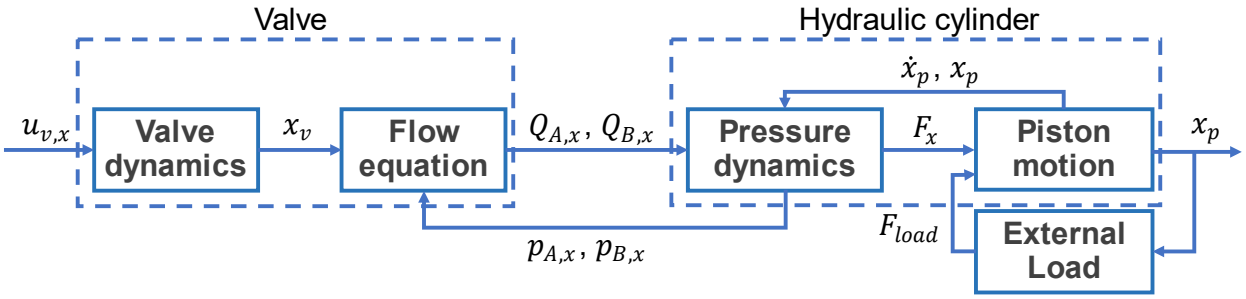

Fig. 3. Overall structure of the simulation model that describes the dynamic behaviour of the machine support in x direction

Valve. Depending on the input voltage u_v, the spool inside the valve is moved to its relative position x_V (range: 0% to ±100% opened). The temporal relationship between u_V and x_V (valve dynamics) is simply described by a second order transfer function according to [5]. The spool position x_V mainly influences the volume flow through the valve Q_A and Q_B from the pump to cylinder chamber A or B. Q_A and Q_B are modelled according to the data sheet with a kinked flow characteristics and zero lapping via an orifice equation. Thus, the volume flow is a function of the actual pressures inside of the cylinder chambers p_A and p_B.

Hydraulic cylinder. The pressures inside the cylinder p_A and p_B are calculated based on the continuity equation for each cylinder chamber. Taking the compressibility of the oil into account, the pressure rates $\dot{p}_A$ and $\dot{p}_B$ and thus the pressures inside of the cylinder are described by dynamic pressure differential equations taken from [8]. From p_A and p_B, a resulting force $F = A_{p,A}p_A - A_{p,B}p_B$ acts on the piston side faces $A_{p,A}$ and $A_{p,B}$ that accelerates piston mass m_p and that leads to a piston motion. Additionally, it assumed that the cylinder is loaded by an external force F_{ext}. Based on Newton's second law, the motion equation of the piston is thus formulated to:

$$m_p\ddot{x}_p = A_{p,A}p_A - A_{p,B}p_B - F_{ext}. \quad (1)$$

External force. The external force consists of friction forces F_{fric} and, in case of flow forming, of the forming forces F_{load}. The friction force is assumed to be constant at a value of F_{S0} and is directed opposite to the cylinder motion. This fact is incorporated in Eq. (2) by the term $sign(\dot{x}_p)$.

$$F_{ext} = F_{fric} + F_{load} = F_{S0} \cdot sign(\dot{x}_p) + F_{load}(\Delta r, f) \quad (2)$$

During positioning before or after the forming operation, F_{ext} is exclusively comprised by the friction forces F_{fric}. By contrast, during workpiece production, the roller and consequently the

piston is exposed to mechanical load due to the forming forces F_{load}. Note that the axial and radial forming forces are different to each other, so $F_{load,x}$ differs from $F_{load,y}$. The forces are assumed to be a static, nonlinear function $F_{load}(\Delta r, f)$ depending on infeed $\Delta r \sim y_p$ and feed rate $f = \dot{x}_p$.

Parameter identification

To simulate the previously described model, it is required to determine the model parameters in advance. For this purpose, the model equations are fitted with S*imulink Parameter Estimator Toolbox* to measured step response data from the forming machine using nonlinear least square algorithm. Additionally, the natural frequency of the cylinder was identified from the measurements and in consequence the piston mass m_p (according to [9]). However, this procedure is not suitable for building the function $F_{load}(\Delta r, f)$ in Eq. (2) since it is a complex nonlinear function that not only depends on the machine but also on the flow forming process. Thus, additional flow forming experiments are required for the parameter identification.

Identification of the forming forces F_{load} (external load model). A systematic, full factorial experimental study was carried out on the single roller machine. Workpieces were manufactured investigating 15 different parameter combinations (5 levels of feed rate from 0.1 to 0.5 mm/s and 3 infeed levels from 1 to 3 mm). During the experiments, the pressures were recorded and the hydraulic force for each cylinder was calculated by $F = p_A A_{p,A} - p_B A_{p,B}$. Since the forming forces are much higher than the friction force, it can be assumed that the calculated force F directly corresponds to F_{load}. For the evaluation, $F_{load,x}$ in axial and $F_{load,y}$ in radial direction were averaged over time and plotted against the process parameters (see Fig. 4).

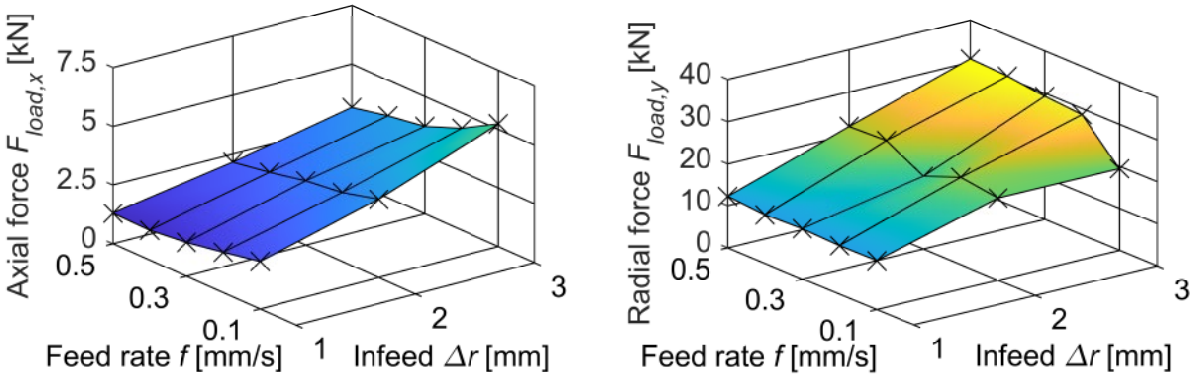

Fig. 4. Meas. forming forces (load) during flow forming for different process parameters

It is notable, that the radial forces (y direction) are much higher than the axial (x direction) for each process parameter combination. In x direction, the forming force is in a range of approx. 1.5 to 6 kN. By contrast, the forces in y direction are in a range of 10 to 30 kN. In x as well as in y direction, the measured forces depend on the process parameters used in the respective experiment, i.e. the feed rate f $(= \dot{x}_p)$ and the infeed Δr $(\sim y_p)$. In x direction, the measured $F_{load,x}$ is higher if the feed rate f is low, or if the infeed Δr is high. In y direction, $F_{load,y}$ clearly rises the higher the infeed Δr is. Additionally, the force is reduced by lowering the feed rate. To include the described empiric dependency on process parameters in the model, the measurement results from Fig. 4 are modelled by an empiric lookup table F_{load}.

Control design

A special closed-loop control concept for the hydraulic actuators was developed due to the special use in the flow forming process. Since flow forming depends on axial feed rate $f = \dot{x}_p$ and on the infeed $\Delta r \sim y_p$, the closed-loop control must be able to control both

- the piston positions x_p and y_p

Materials Research Proceedings 41 (2024) 1426-1435 https://doi.org/10.21741/9781644903131-158

- the position velocities $\dot{x}_p$ and $\dot{y}_p$.

The piston positions x_p and y_p are coordinates of discrete points on the roller trajectory. The roller trajectory consists of multiple points and the roller should linearly move on a straight line from point to point with the position velocities $\dot{x}_p$ and $\dot{y}_p$. The piston positions and velocities at or between the discrete points serve as desired values for the control. The desired values are stored in a matrix P that is similar to a G-Code program of an industrial CNC control.

$$P = \begin{bmatrix} x_{p,des,1} & \dot{x}_{p,des,1} & y_{p,des,1} & \dot{y}_{p,des,1} \\ \vdots & \vdots & \vdots & \vdots \\ x_{p,des,m} & \dot{x}_{p,des,m} & y_{p,des,m} & \dot{y}_{p,des,m} \end{bmatrix} \tag{3}$$

Each row corresponds to the desired positions $x_{p,des,i}$ and $y_{p,des,i}$ at a discrete point i that should be reached from the previous point $x_{p,des,i-1}$ and $y_{p,des,i-1}$ by velocity $\dot{x}_{p,des,i}$ and $\dot{y}_{p,des,i}$. If the desired position is met, then the next row is applied, so $x_{p,des,i+1}$, $y_{p,des,i+1}$, $\dot{x}_{p,des,i+1}$ and $\dot{y}_{p,des,i+1}$ becomes to be the actual desired value. The desired values are optionally corrected by the closed-loop property control and then committed the control unit of the cylinder (see Fig. 5).

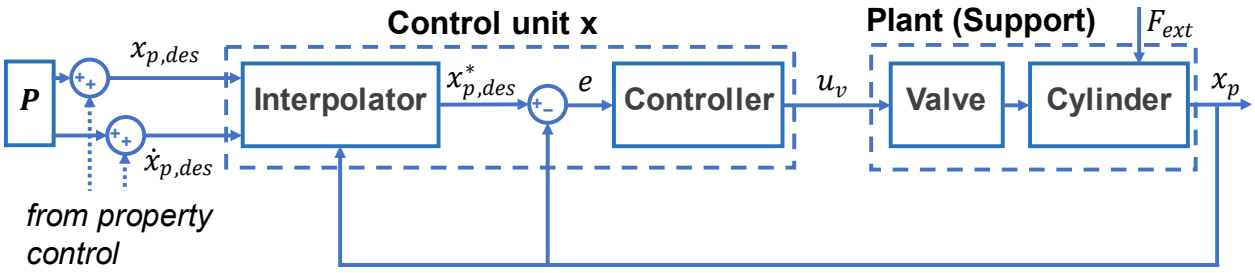

Fig. 5. Closed-loop control structure for the X axis

At first, the desired values are processed in an interpolator that calculates the desired value $x^*_{p,des}$ or $y^*_{p,des}$ for the controller. The interpolator equation for the x axis is given by Eq. (4).

$$x^*_{p,des} = \begin{cases} x_{p,des} & \text{if } |x_{p,des} - x_p| < \varepsilon \\ sign(x_{des} - x_p) \cdot \dot{x}_{p,des} \cdot (t - t_0) + x_0 & \text{else} \end{cases} \tag{4}$$

If the actual piston position x_p is within a distance of threshold ε (here: 0.1) to the $x_{p,des}$ from matrix P, then $x_{p,des}$ also acts as desired value $x^*_{p,des}$ for the controller. In this case, the control behaves like a conventional position control. If not, a fictional desired value is interpolated from processing the velocity $\dot{x}_{p,des}$ and starting from value x_0. Note, that x_0 is the actual piston position, when the control switches into the next row of P or if there is a control action of the superior closed-loop property control, at time t_0. Thus, the complex problem of controlling both position and velocity is reduced to a simple position control task. Following to the interpolator, $x^*_{p,des}$ is compared to the actual piston position x_p or y_p by Eq. (5) and processed by the position controller.

$$e_x = x^*_{p,des} - x_p \qquad e_y = y^*_{p,des} - y_p \tag{5}$$

The position controller is realized with a PI controller that includes a proportional gain $K_{p,x}$ and an integral gain $K_{i,x}$ for the x axis and gains $K_{p,y}$ and $K_{i,y}$ for the y axis. The controller outputs a voltage $u_{v,x}$ or $u_{v,y}$ to the valves of the real system or – in case of the model – to the valve model.

Controller parameterization. The parameters of the position controller were determined by linearizing the plant model using *Simulink Model Linearizer* and analyzing the system dynamics in frequency domain concerning the gain and phase margin. The selected controller gains should lead to closed-loop control dynamics which are as fast as possible, but also stable. Thus, Nyquist stability criterion [10] was applied and the gains were chosen to those values shown in Table 1.

Table 1: Model-based identified controller gains

		X direction	Y direction
Proportional gain	K_p	0.8	0.7
Integral gain	K_i	0.4	0.54

The closed-loop controller gains were additionally tested by analyzing their performance in time using the simulation model. For this test, $x^*_{p,des}$ and $y^*_{p,des}$ were changed stepwise (±1 mm and ±2 mm) in the model and the response of the piston positions x_p and y_p was recorded (Fig. 6).

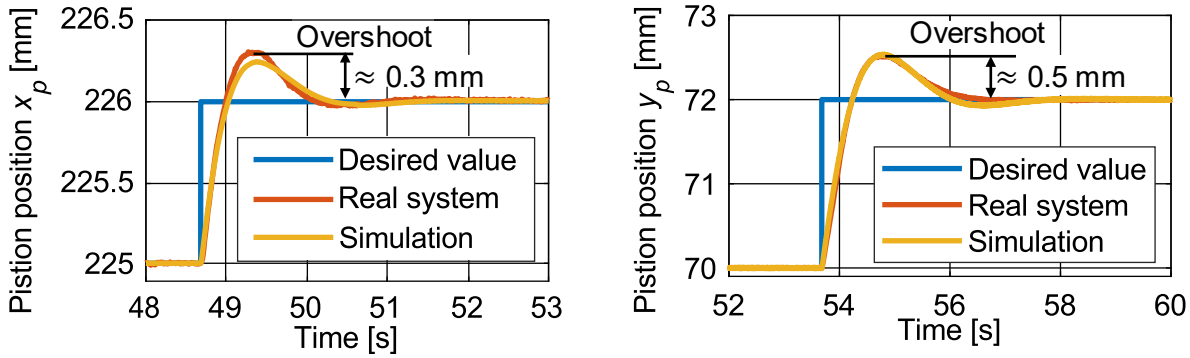

Fig. 6. Controller test by step response (example: height 1 mm in x and 2 mm in y direction)

As shown in Fig. 6, the desired values in x and y direction are controlled stable and stationary in the simulation. The system response includes a slight, well-damped overshoot of max. 0.5 mm that is acceptable to get a faster system response. Thus, the controller parameters from Table 1 are successfully proofed to be suitable for the final closed-loop control at the flow forming machine.

For this reason, the total control concept including the controllers was adapted to LabVIEW and integrated in the machine control of the flow forming machine. Then, the controllers of the closed-loop position control were commissioned by repeating the step response performance test that was already performed virtually in MATLAB with the model. According to Fig. 6, the dynamic behavior of the closed-loop position control is in a good agreement with the model.

Experimental control validation

The proposed control concept (interpolator and closed-loop position control) was finally validated at the actual flow forming machine. For this purpose, experiments with and without load were performed using axial and redial velocities $\dot{x}_{p,des}$ and $\dot{y}_{p,des}$ from 0,01 mm/s (extremely slow flow forming) to 18 mm/s (rapid traverse without flow forming). The core of these experiments was the manufacturing of 5 workpieces by flow forming with feed rates $f = \dot{x}_{p,des}$ from 0.1 mm/s to 0.5 mm/s and an infeed Δr of 2 and 3 mm ($y_{p,des}$ = 141 mm and $y_{p,des}$ = 142 mm). In the following, the validation results concerning the accuracy of the control will be deeper analyzed taking the example of the experiment Δr = 2 mm and f = 0.1 mm/s (see Fig. 7). This experiment is divided into three phases: prepositioning in x direction without load (I), prepositioning in y direction without (II) and the actual flow forming operation with load (III). During I, the x axis is moved from x_p = 1 mm to 325 mm within 46.28 s. Thus, the actor movement corresponds very good to the desired value. During this time, the y axis is kept on a constant position of y_p = 1 mm (measured mean value 1.001 mm). Subsequently, the y axis is prepositioned to y_p = 141 mm, that corresponds to an infeed of Δr = 2 mm to the workpiece, within 35 s. The result is also in a good agreement with the desired value since $\dot{y}_{p,des}$ was set to 4 mm/s. In the last phase, the workpiece is manufactured by an axial movement with $f = \dot{x}_{p,des}$ = 0.1 mm/s while the actuator position in y direction is kept constant. This phase is the most critical due to the external load from plastic deformation during flow forming which might force the actuators out of their desired position.

Nevertheless, the measured, actual actuator behavior is conform with the desired despite of the load. The average value of $\dot{x}_p$ is actually 0.1 mm/s and y_p is 140.999 mm. By taking a deeper look on the measurement of y_p, it can be seen that the impact of the load on the actuator position results only in a slight oscillation of ±0.005 mm which is significantly less than known from experiments with the flow forming machine before.

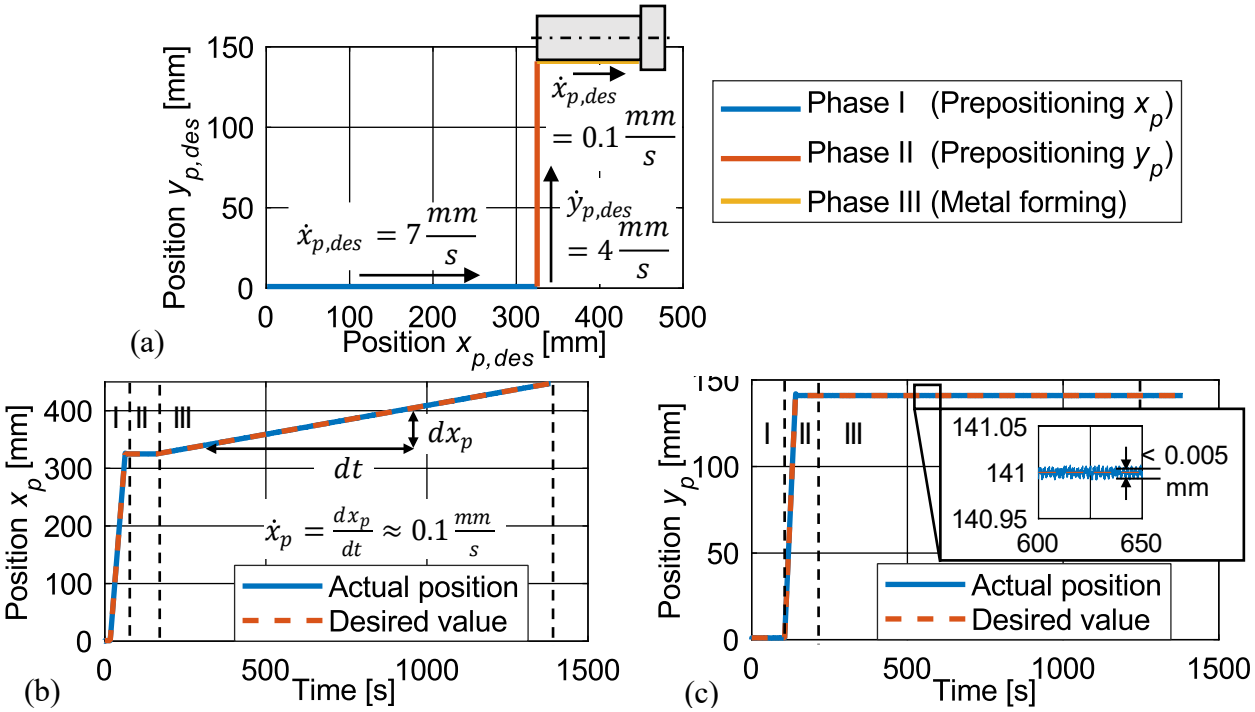

Fig. 7. Desired and actual actuator position during flow forming (Δr = 2 mm, f = 0.1 mm/s).

These measurements are also confirmed by the other experiments. To analyze the impact of the control results, the manufactured specimens were measured with MarSurf M300 and the average roughness R_a was compared to specimens produced at the single roller machine in the past (from [3]), see Fig. 8. In the figure, additionally the measured R_a of specimens manufactured on a three roller flow forming machine (Bohner & Koehle BD 40) is shown. Those specimens were a part of a DOE in [11]. For a better comparison, workpieces were chosen which were manufactured with an identical feed rate and a strain similar to the new specimens from single roller flow forming.

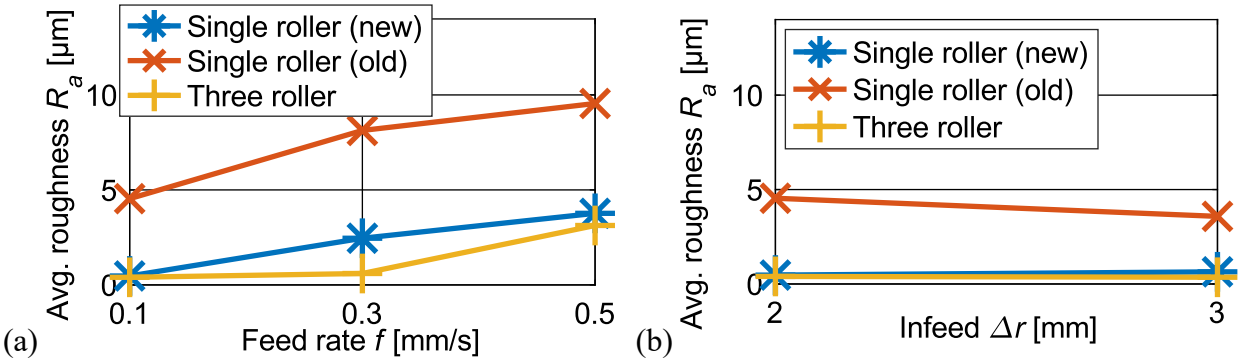

Fig. 8. Average roughness R_a of workpieces manufactured on the single roller machine with the old and new actuator control in comparison to an industrial three roller flow forming machine, for: (a) constant Δr = 2 mm, (b) constant f = 0.1 mm/s

Fig. 8 shows that with the new control, R_a is significantly reduced by a factor of >3 compared to the old single roller results from [3]. Due to the control enhancement, R_a is minimum 0.47 µm

at $f = 0.1$ mm/s and rises with increasing feed rate up to 3.768 µm (for $\Delta r = 2$ mm). Thus, the roughness R_a in single roller flow forming is now almost on the same level as in three roller flow forming. There, R_a is 0.47 µm in the case of $f = 0.1$ mm/s and $\Delta r = 2$ mm, for example. The similarity of the roughness in single roller flow forming and three roller flow forming is remarkable since the workpiece is more often overrolled with three rolls. Thus, a sincere added value concerning the workpiece quality in single roller flow forming is offered by the enhanced process parameter tracking with the new control.

Conclusion

A novel closed-loop control for a hydraulic single roller flow forming machine was model-based developed and validated in this paper. Due to model-based procedure to design the control, it became possible to create a control that is able to accurately keep the desired position and velocity despite of the high forming forces due to flow forming. Thus, the developed control features the desired functionality to accurately control both the actuator position and velocity in the flow forming process. As shown during the validation, it is consequently possible to manufacture workpieces on the single roller flow forming machine with a better surface quality. The surface roughness of the manufactured parts is now even in a similar range to that of conventional machines with three rollers. Hence, the flow forming machine including the novel actuator control is now predestined to be prospectively used in the closed-loop property control. The closed-loop property control of the α'-martensite fraction and wall thickness reduction has already been proposed by the authors in [1]. It includes a so-called soft sensor for the online determination of the α'-martensite. However, the soft sensor accuracy is hardly depending on the surface roughness (see [3]). For this reason, it is expected that the α'-martensite can also be set with an increased accuracy due to the proposed actuator control presented in this paper.

Acknowledgement

The authors would like to thank the German Research Foundation (Deutsche Forschungsgemeinschaft, DFG) for their support of the depicted research within the priority program SPP 2183 "Property-controlled metal forming processes", through project no. 424335026 "Property control during spinning of metastable austenites".

References

[1] L. Kersting, B. Arian, J. Rozo Vasquez, A. Trächtler, W. Homberg, F. Walther, Echtzeitfähige Modellierung eines innovativen Drückwalzprozesses für die eigenschaftsgeregelte Bauteilfertigung, at – Automatisierungstechnik 71:1 (2023) 68–81. https://doi.org/10.1515/auto-2022-0106

[2] B. Arian, W. Homberg, L. Kersting, A. Trächtler, J. Rozo Vasquez, F. Walther, Produktkennzeichnung durch lokal definierte Einstellung von ferromagnetischen Eigenschaften beim Drückwalzen von metastabilen Stahlwerkstoffen, in: G. Hirt (ed.), 36. Aachener Stahlkolloquium – Umformtechnik "Ideen Form geben", Aachen, 2022, pp. 333–347

[3] J. Rozo Vasquez; L. Kersting; B. Arian; W. Homberg; A. Trächtler; F. Walther: Soft sensor model of phase transformation during flow forming of metastable austenitic steel AISI 304L. Numerical Methods in Industrial Forming Processes: Numiform 2023, Springer LNME. *in press.*

[4] S. Rost, Entwurf, Analyse und Regelung einer kinematisch redundanten Roboterstruktur mit hydraulischen Antrieben variabler Nachgiebigkeit, Doctoral Dissertation, TU Braunschweig, 2016. https://doi.org/10.24355/dbbs.084-201606290936-0

[5] S. Knoop, Flachheitsbasierte Positionsregelungen für Parallelkinematiken am Beispiel eines hochdynamischen hydraulischen Hexapoden, Doctoral Dissertation, Paderborn University, Heinz Nixdorf Institut, Paderborn, 2016. https://doi.org/10.17619/UNIPB/1-99

[6] D. Hornjak, Grundlegende Untersuchungen der Prozess- und Werkzeugparameter und ihre Wechselwirkungen für das thermo-mechanisch unterstützte inkrementelle Umformverfahren des Reib-Drückens, Doctoral Dissertation, Paderborn University, Shaker, Aachen, 2013.

[7] B. Lossen, Ein Beitrag zur Herstellung von hybriden Bauteilen mittels Reibdrücken, Doctoral Dissertation, Paderborn University, Shaker, Düren, 2019.

[8] L. Kersting, B. Arian. J. Rozo Vasquez, A. Trächtler, W. Homberg, F. Walther, Innovative online measurement and modelling approach for property-controlled flow forming processes. Key Engineering Materials 926 (2022) 862–874. https://doi.org/10.4028/p-yp2hj3

[8] J. Jelali, A. Kroll, Hydraulic Servo-systems – Modelling, identification and control, Springer, London, 2003, DOI 10.1007/978-1-4471-0099-7

[9] S. Helduser (Ed.), O+P-Fachlexikon "Fluidtechnik von A bis Z" (O+P technical glossary "Fluid technology from A to Z"), HAWE Hydraulik, Aschheim, read on https://www.hawe.com/ fluid-lexicon/, the 08th February 2024.

[10] H. Nyquist, Regeneration theory, Bell System Technical Journal 11:1 (1932) 126-147. https://doi.org/10.1002/j.1538-7305.1932.tb02344.x

[11] B. Arian, W. Homberg, J. Rozo Vasquez, F. Walther, M. Riepold, A. Trächtler, Forming metastable austenitic stainless steel tubes with axially graded martensite content by flow-forming, ESAFORM 2021 24th International Conference on Material Forming Liège (2021). https://doi.org/10.25518/esaform21.2759